Journal of

Applied and Computational Mechanics

Shahid Chamran
University of Ahvaz

Research Paper

Potential of Semi-Empirical Heat Transfer Models in Predicting the Effects of Equivalence Ratio on Low Temperature Reaction and High Temperature Reaction Heat Release of an HCCI Engine

Masoud Rabeti[1], Omid Jahanian[2], Ali Akbar Ranjbar[3], Seyed Mohammad Safieddin Ardebili[4], Hamit Solmaz[5]

[1] Department of Mechanical Engineering, Babol Noshirvani University of Technology, Babol, Iran, Email: masoud.rabeti@gmail.com

[2] Department of Mechanical Engineering, Babol Noshirvani University of Technology, Shariati Av, Babol, 4714873113, Iran, Email: jahanian@nit.ac.ir

[3] Department of Mechanical Engineering, Babol Noshirvani University of Technology, Babol, Iran, Email: ranjbar@nit.ac.ir

[4] Department of Biosystems Engineering, Shahid Chamran University of Ahvaz, Ahvaz, Iran, Email: m.safieddin@scu.ac.ir

[5] Automotive Engineering Department, Faculty of Technology, Gazi University, Ankara, Turkey, Email: hsolmaz@gazi.edu.tr

Abstract. In this paper, the influence of equivalence ratio on the low-temperature reaction heat release (LTR-HR) and high-temperature reaction heat release (HTR-HR) of homogeneous charge compression ignition engine has been experimentally and numerically examined. The numerical study was performed using zero-dimensional (0D) single-zone model by considering the chemical kinetic of fuel combustion. Annand, Woschni, Hohenberg, Chang (Assanis), and Hensel semi-empirical heat transfer models were employed in the 0D single-zone simulations. In this study, the in-cylinder pressure, rate of heat release, LTR-HR and HTR-HR were investigated. The Hensel heat transfer model was the only model that predicted the combustion in all of the operating conditions. The Hohenberg model properly recognized the effects of equivalence ratio changes on the HTR-HR.

Keywords: HCCI Combustion, Zero-Dimensional Single-Zone Model, Semi-Empirical Heat Transfer Models, Low Temperature Reaction Heat Release, High Temperature Reaction Heat Release, Equivalence Ratio.

1. Introduction

The industrial development of the world has led to increased fuel consumption and higher amounts of emissions. Nowadays, in most cases, the compression ignition (CI) and spark ignition (SI) engines provide the necessary power for transportation around the world. The power production in these engines is done based on the reciprocating movements of piston. Still the key differences in the performance of these engines are the fuel consumption rate, efficiency, and emissions. The most critical issues in the design of internal combustion engines (ICEs) are increasing their efficiency, reducing their fuel consumption and emissions. These issues have been considered in the low-temperature combustion (LTC) engines [1, 2].

The LTC engine is a novel technology that combines the performance of CI and SI engines. One variant of LTC engines is a Homogeneous Charge Compression Ignition (HCCI) engine. In HCCI engines, similar to SI engines, fuel/air mixture is used; however like CI engines, these engines work based on the compression ignition. Due to high thermal efficiency, and insignificant amounts of soot and NOx emissions in HCCI engines, the combustion in these engines has attracted much attention in the last decade. Considering the various applications of ICEs in the land or sea transportations, and also, their usage in power production, HCCI engines have a great potential in reducing greenhouse gases and other emissions. These advantages are obtained due to the entrance of a premixed and lean mixture into the combustion chamber, and its auto-ignition with the produced heat from compression. Despite extensive research in this area, there are still some problems with HCCI engines, such as limited operating range and the uncontrolled start of combustion (SOC). Also, because of the low combustion temperatures in these engines, carbon monoxide (CO) and unburnt hydrocarbon (UHC) and emissions are important [3- 5].

Usually, for evaluating and optimizing the performance of the engine in different operating conditions, investigating the influential parameters on the combustion, performing the energy analysis, and controlling the combustion process, the engine simulation programs are used. One of the ways to simulate the HCCI engines is using a zero-dimensional single zone (0D-SZ) model, which requires some methodologies for solving the mass and energy equations. In these models, the entire combustion

chamber is considered as a uniform temperature/pressure zone, and also chemical kinetics are used for solving the combustion equation. One of the sub-models of the energy equation is the heat transfer model, which estimates the amount of heat transfer between cylinder wall and in-cylinder charge. Considering the significant temperature dependence of auto-ignition in HCCI engines, and the considerable influence of heat transfer on the simulation results, the selection of the proper heat transfer model is very significant [6, 7].

The idea of using HCCI engines traced back to Onishi et al. [8] in 1979; however, this technology is still under development. So, simulating these engines can lead to extending their operational range, enhancing their operating condition and reducing their emissions.

Numerous experimental studies have been carried out on HCCI engines so far. Extending the operating condition of these engines and using different fuels for reducing the fuel consumption and emissions were the most essential objectives in these studies.

The effects of different fuels in the HCCI engines were examined by Kim and Lee [9]. In their research, diesel, gasoline, and n-heptane fuels were employed. These researchers studied different phases of combustion in their work. Ebrahimi and Desmet [10] evaluated the effects of engine speed and residual gas from the previous cycle on the combustion phase of HCCI engines. The results of this study showed that the temperature, dilution of the mixture, and composition of the residual gases could affect the combustion duration in the next cycle. The impacts of iso-propanol and n-heptane fuel mixture on the combustion characteristics of an HCCI engine and its performance was analyzed by Ipci et al. [11]. In their research, it was concluded that increasing iso-propanol delays the SOC, while it reduces the combustion duration. The influence of the air inlet temperature on the combustion, engine performance and emission characteristics of an HCCI engine was evaluated by Cinar et al. [12]. In that study, gasoline fuel was employed. The results represented that a higher air inlet temperature increases the rate of heat release (RoHR) and the in-cylinder pressure, while it reduces the combustion duration. Cinar et al. [13] analyzed the impacts of valve lift on the combustion in an HCCI engine with gasoline fuel. They revealed that with the low lift cams, the operating range of HCCI engines can be extended in the knocking and misfiring operating zones. The impact of the compression ratio on the combustion in the HCCI engines was studied in the work of Calam et al. [14]. The results of their research suggested that by increasing the compression ratio, the combustion duration decreases. Also, it was shown that by increasing the octane number of the fuel, the combustion duration increases. The effects of injection timing in an n-heptane-fueled HCCI engine were evaluated by Polat et al. [15]. It was found that earlier injection, increases the maximum pressure and advances the SOC.

Among the carried out 0D studies in the field of HCCI engines, these research papers can be indicated. Jahanian and Jazayeri [16] investigated the influences of adding formaldehyde on the performance of an HCCI engine with Compressed Natural Gas (CNG) fuel through 0D-SZ simulations. These researchers used a thermodynamic model, which included detailed chemical kinetics, and they revealed that the hydroxyl radical has a considerable influence on the combustion of the CNG. Besides, based on their results, the addition of the formaldehyde can affect the operating range of the engine. Fathi et al. [17] examined the 0D-SZ and multi-zone simulations of an HCCI engine. The results represented that the single-zone model could efficiently predict SOC, but for the RoHR, the multi-zone model should be used. The energy and exergy analysis of a HCCI engine fueled with hydrogen was carried out by Namar and Jahanian [18] by means of the 0D-SZ thermodynamic model. In their study, they examined the impacts of engine input parameters with the 0D-SZ model coupled with the detailed chemical kinetic. The results indicated that the Inlet Valve Closing (IVC) pressure and the equivalence ratio have the greatest effect on the exergy and the irreversibility. The most important issue that has been considered in this paper is the heat transfer models in thermodynamic modeling. The semi-empirical models present the instantaneous convection heat transfer coefficient in the same way as the steady heat transfer correlations for the flow over a flat plate or inside a tube. The investigation on the semi-empirical heat transfer correlations was started by Nusselt [19] in 1923, and the presented correlation by Nusselt became the basis of the subsequent studies. The semi-empirical heat transfer models are correlations that are used to calculate the average heat flux as a function of the crank angle. Annand [20] was one of the first researchers who developed a useful model for modeling the heat transfer in CI and SI engines. In the presented model by Annand, the quasi-steady heat transfer process and the rate of heat transfer were considered as functions of the temperature difference between the working fluid and the cylinder wall. Also, in this model, the uniform distribution assumption of the in-cylinder gas was considered. Woschni [21] presented one of the most useful correlations for calculating the heat transfer in the ICEs. The presented model by Woschni was based on the similarity law of the steady heat transfer. The basis of the Woschni model was the same correlation that was presented by Nusselt [19]. After examining the effects of different parameters and performing numerous tests, Woschni presented his correlation. One of the other utilizable models is the Hohenberg model [22]. Hohenberg developed his model by modifying the Woschni model. The modifications included some changes in the characteristic length and characteristic velocity. Moreover, Bergende [23] modified the Woschni model with a different approach. He presented his correlation by separating the control volume into two zones of burnt and unburnt. He also used a different characteristic length and characteristic velocity in his model. Cheng et al. [24] developed a model for HCCI engines by modifying the Woschni model. This model is also known as the Assanis model. These researchers presented their correlation for the HCCI engines by changing the exponent of different parameters, selecting the instantaneous height of the combustion chamber as the characteristic length, and altering the characteristic velocity of the Woschni model. One of the other presented correlations for the HCCI engines was developed by Hensel et al. [25]. These researchers developed a proper model for the HCCI engines by modifying the Annand model. Different studies have concentrated on the effects of using these models. Soyhan et al. [26] studied the performance of different heat transfer models for the HCCI engines. These researchers used the enhanced Trice engine simulation code to model the single-cylinder Ricardo Hydra research engine in the HCCI operating state. They used the Woschni, Hohenberg, and Assanis correlations for evaluating the performance of HCCI engines, and compared their results with the experimental data. Broekaert et al. [27] tested different semi-empirical heat transfer models for HCCI engines. These researchers used Thin Film Gauge (TFG) sensors to measure the heat flux experimentally. In another experimental research by Broekaert et al. [28], the influence of the engine setting was investigated on the wall heat flux in an HCCI engine. They used n-heptane fuel, and they evaluated the spatial variation in their work. The heat transfer measurements on the cylinder wall and head showed a small spatial variation in the heat flux in the combustion chamber. In another investigation which was conducted by Broekaert et al. [23], the semi-empirical heat transfer models were evaluated for the combustion in the HCCI engines. In their study, the changes in the heat flux, the heat loss, and the maximum heat flux were examined by the studied semi-empirical heat transfer models in different operating conditions.

So far, different studies have been conducted on investigating the effects of various parameters in HCCI engines. To the best of the authors' knowledge, there is not a study that specifically concentrated on the capabilities of 0D-SZ models, especially semi-empirical heat transfer models for predicting the influence of the equivalence ratio on the LTR and HTR heat release in the HCCI engines. Therefore, this research aims to experimentally and numerically study this subject. The numerical study is carried out using the 0D-SZ models by considering the chemical kinetics. In the 0D-SZ simulations, the Annand, Woschni, Hohenberg, Chang (Assanis), and Hensel semi-empirical heat transfer models were employed.

Table 1. The specifications of the test engine.

Number of cylinders	1
Bore (mm)	80.26
Stroke (mm)	88.90
Compression ratio	5:1 – 13:1
Fuel injection system	Port injection
IVO	12 °CA BTDC
IVC	56 °CA ABDC
EVO	56 °CA BBDC
EVC	12 °CA ATDC

Table 2. The engine configurations for the tests.

Test no.	Engine speed (rpm)	Equivalence ratio	Test no.	Engine speed (rpm)	Equivalence ratio
1	800	0.31	9	1200	0.34
2	800	0.39	10	1200	0.4
3	800	0.5	11	1200	0.53
4	800	0.62	12	1200	0.58
5	1000	0.32	13	1400	0.35
6	1000	0.41	14	1400	0.41
7	1000	0.54	15	1400	0.46
8	1000	0.61	16	1400	0.55

2. The Experimental Setup and Procedures

In this section, the condition of the studied system, equipment, measuring technique, data collection, and the analytical methods will be explained.

2.1 The experimental setup

In this research, a four-stroke single-cylinder Ricardo Hydra test engine with a variable compression ratio was used. This engine was an SI engine that was transformed into an HCCI engine. The specifications of this engine have been presented in Table 1, and Fig. 1. demonstrates the schematics of the experimental setup.

In the performed experiments, the injection system sprayed the fuel into the intake port. A fuel control system embedded on the control panel, adjusted the amount of fuel. The equivalence ratio was kept constant; using a system including a potentiometer. The potentiometer measured the injector spray characteristics and the fuel consumption. Equipment calibration was carried out before tests. The engine was connected to an electrical type dynamometer (McClure brand); with nominal power of 30 kW @6500 rpm. Inlet air temperature was controlled with a controller placed in the connection part between suction engine block and suction manifold. This closed cycle controller connected to the electrical control panel, adjusted the inlet air temperature via K-type thermocouple installed behind the heating system. In-cylinder pressure was recorded every 0.36 crank angle degree via Kistler 6121 piezoelectric pressure sensor. An encoder made it possible to recognize piston position in this interval. Cussons P4110 combustion analysis device was used to log data and a National Instrument USB 6259 data collection card, converted the data to digital signals. The pressure data was averaged for 50 consecutive cycles in every test. As an initial conditioning, it was measured that in HCCI operating mode, the temperature of cooling water was fixed on 343K, while the temperature of oil was fixed on 333K. These were considered as the operating temperatures of the HCCI combustion. In the principle tests, the engine was started in SI mode, and when HCCI operating temperatures Achieved, ignition system was tuned off and the combustion automatically switched to HCCI. Cooling water and lubricating oil temperatures were kept constant for balanced performance. For the experiments, gasoline with a mixture of 20% isooctane (C_8H_{18}) and 80% n-Heptane (C_7H_{16}), obtaining octane number of 20, was utilized. The tests were carried out in various engine speeds (N=800, 1000, 1200, and 1400 rpm), with different value for equivalence ratios. In the 16 studied operating states, the inlet air temperature and the compression ratio were kept constant at 313K and 12, respectively. The accuracy of pressure sensor and exhaust gas analyzer for equivalence ratio were ±0.5% and 0.001, respectively. Also, the sensitivity scale of the fuel tank was 0.01 g. The engine configurations for these 16 operating states have been tabulated in Table 2.
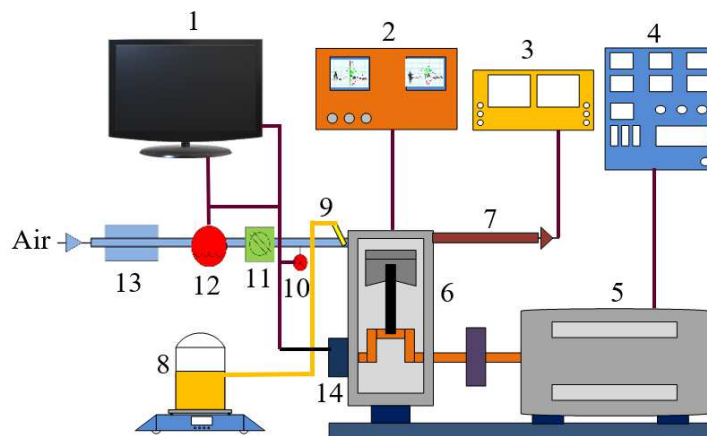

Fig. 1. 1- Computer, 2- Combustion analysis device, 3- Gas analyzer, 4- Dynamometer control, 5- DC Dynamometer, 6- HCCI engine, 7- Exhaust, 8- Fuel tank, 9- Injector, 10- Thermocouple, 11- Throttle valve, 12- Air heater, 13- Air flow measurement device, 14- Encoder.

2.2 Combustion analysis method

A MATLAB code was developed to average 50 consecutive pressure data and calculate in-cylinder pressure, the rate of changes of cylinder volume, RoHR, and start of LTR-HR and HTR-HR via pressure trend. RoHR was calculated based on the first law of thermodynamics using eq. (1). [29]:

$$\frac{dQ}{d\theta} = \frac{\gamma}{\gamma - 1} P \frac{dV}{d\theta} + \frac{1}{\gamma - 1} V \frac{dP}{d\theta} + \frac{dQ_{heat}}{d\theta} \tag{1}$$

where $dQ/d\theta$ is the gross heat release rate (RoHR) and P shows the in-cylinder pressure which calculated by using the MATLAB algorithm, and V is the volume of the cylinder and is calculated with the relation of combustion chamber volume which is defined in classic engine text [29]. Also, $d\theta$ denotes the changes in the crank angle, γ shows the specific heat ratio C_p/C_v and calculated using CANTERA module in the MATLAB software for each time step. Last term of the Eq. (1) is $dQ_{heat}/d\theta$, representing the heat transfer from the charge to the cylinder wall and could be obtained by eq. (2).

3. The Numerical Approach and Procedure

The assumptions of this modeling method were as follows:
- In the combustion chamber, the temperature, pressure, and all of the mixture properties are homogenous in every moment.
- The mixture in the combustion chamber is considered as an ideal gas mixture.
- The simulation of the closed cycle of combustion starts from IVC and continues until EVO.
- Semi-empirical correlations are used for modeling the heat transfer between the charge in the combustion chamber and the cylinder wall.

The schematic of the 0D-SZ model of the HCCI engine has been illustrated in Fig. 2. [30].

In this model, the energy conservation equation, the mass conservation (chemical species), the ideal gas equation of state, and the volume changes in the combustion chamber are simultaneously solved. Considering that these equations are presented in numerous references [16, 31, 32], this paper only indicates the semi-empirical heat transfer models, which were the focus of this research.

The semi-empirical heat transfer models demonstrate the heat transfer from the combustion chamber to the cylinder walls as the convective heat transfer. This assumption is right when there are no soot particles in the combustion chamber. Because, if there are soot particles, the radiation heat transfer should be considered as well. The soot emission level is insignificant in HCCI engines; also, the heat transfer is assumed in a quasi-steady state. The heat transfer equation can be written as follows [23]:

$$Q_{convection} = hA(T_{gas} - T_{wall}) \tag{2}$$

in which, h is the coefficient of convective heat transfer, heat transfer area (A), and ΔT shows the temperature difference between the gas and the cylinder walls. Generally, the semi-empirical models present a correlation for the convective heat transfer coefficient. All of the models are based on Pohlhausen's equation [23], which expresses the convective heat transfer on a flat plate using the theory of boundary layer [23]:

$$Nu = a.Re^b.Pr^c \tag{3}$$

where Nu shows the Nusselt number, Re represents the Reynolds number, and Pr indicates the Prandtl number. Also, a, b, and c are the model coefficients [23].

The Prandtl number does not significantly change for most of the fuels in the engine cycle [33]; thus, it is combined with the 'a' scaling coefficient. As a result, the convective heat transfer coefficient is acquired as a function of the characteristic velocity (V), characteristic length (L), viscosity (μ), thermal conductivity (k), and the charge density (ρ) [20].

$$h = aV^b L^{b-1} k \mu^{-b} \rho^b \tag{4}$$

In this equation, 'a' and 'b' are the model coefficients. The difference between the heat transfer models is in the selection of the velocity and characteristic length, determination of the charge thermal properties, and the model coefficients, which are achieved by matching the model with the experimental data.

Annand developed eq. (4). for obtaining the convective heat transfer coefficient. It is noteworthy that in his equation, he considered the inner diameter of the cylinder (B) as the characteristic length and the mean piston speed (C_m) as the characteristic velocity.
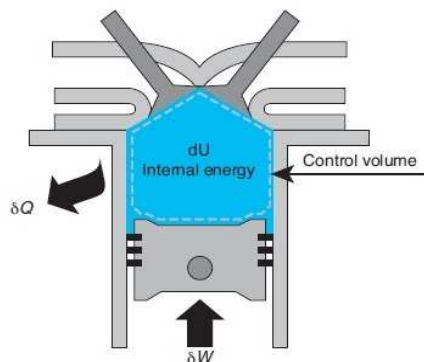

Fig. 2. Schematic of the single-zone model.

By considering and applying the following assumptions on eq. (4)., Woschni presented his correlation [21].

$$1. \rho \sim \frac{P}{T}, 2. k \sim T^{0.75}, 3. \mu \sim T^{0.62} \tag{5}$$

It should be noted that the last two assumptions are only valid for air.
The presented correlation by Woschni is as follows [21]:

$$h = aP^b V^b L^d T^e \tag{6}$$

Woschni selected the inner diameter of the cylinder (B) as the characteristic length, and expressed the following equation as the characteristic velocity [21]:

$$V = C_1 C_m + C_2 \frac{V_s T_r}{P_r V_r}(P - P_0), P_0 = \frac{(\frac{r_c V_d}{r_c - 1})^\gamma P_r}{V^\gamma} \tag{7}$$

In the characteristic velocity equation, C_m is the mean piston speed, P is the instantaneous pressure, V_s is the engine displacement volume, and the r subscript represents the reference point (which is usually considered at the IVC) and P_0 is the motoring pressure. In the combustion and exhaust stages, the C_1 and C_2 coefficients are 2.28 and 0.00324, respectively.

By applying some modifications to the characteristic velocity and characteristic length in Woschni's correlation, Hohenberg proposed his correlation. The presented correlation by Hohenberg is eq. (6).

Hohenberg changed the characteristic length of Woschni's correlation to the diameter of a sphere with the instantaneous cylinder volume. Also, he modified the characteristic velocity to the sum of the piston speed and a constant number. In this model, the characteristic length and the characteristic velocity are $V_{cyl}^{1/3}$ and $C_m+1.4$, respectively. Chang et al. (the Assanis model) modified model of Woschni for the HCCI engines by selecting the instantaneous chamber height as the characteristic length, dividing the C_2 coefficient by 6, and changing the exponent of the temperature (e). These researchers chose the same format of eq. (6). for their model.

In a study, Hensel et al. modified the model of Annand for the HCCI engines. These researchers selected the same presented format in eq. (4). for their model.

The characteristic velocity in the Hensel model is defined as [25]:

$$V = \frac{\sqrt{c_m^2 + c_c^2}}{2} + C_1 \frac{4\dot{m}_{air}}{\pi \rho_{air} B^2}(\frac{h_{IV,WOT}}{h_{IV}})^{C_2} \tag{8}$$

In the characteristic velocity equation, the first term shows the engine speed, and the second term is the velocity of the mixure. The velocity of the mixure is used for applying the effects of the internal residual gas, and the acceleration of the entering flow if a small valve lift (h_{IV}) is used. C_c shows the instantaneous piston speed, $\dot{m}_{air}$ indicates the mean mass flow rate of air, and ρ_{air} represents the air density. Also, h_{IV} and $h_{IV,WOT}$ designate the maximum elevation height of the valve in every operating condition and wide-open throttle state, respectively. Moreover, C_1 and C_2 coefficients are 1.9 and 1.35, respectively, and B indicates the cylinder diameter.

The characteristic velocity, characteristic length, and the coefficients for each of the models have been presented in Tables 3 and 4.

The calculation method for the thermal properties of the mixture is different in the semi-empirical heat transfer correlations. Three different approaches can be used for calculating the thermodynamic properties in the examined models in this study. The first approach, which is for the Annand model, calculates the gas properties in the mean temperature of the mixture (this temperature is achieved from the equation of ideal gas) [20]. The second approach, which is used for the Woschni, Hohenberg, and Assanis (Chang) models, calculates the thermodynamic properties using the correlations for air [24]. The third approach is used by the Hensel model, and it calculates the thermodynamic properties of the mixture applying the correlations for the exhaust gases and air [25]. Based on the conducted research by Broekaert et al. [23], using these three different approaches for calculating the thermodynamic properties of the mixture has an insignificant influence on the calculated heat flux value, therefore, in this study, the thermodynamic properties of the mixture are acquired by means of CANTERA module in the MATLAB software.

To simulate the chemical kinetics, the reduced mechanism was employed, which included 73 chemical species and 296 reactions. This mechanism was previously used for simulating the combustion of different isooctane and n-heptane mixtures in the HCCI engines, and it had acceptable results [34].

Table 3. The characteristic velocity and length in the models

Models	Characteristic Length (L)	Characteristic Velocity (V)
Annand	B	C_m
Woschni	B	$C_1 C_m + C_2 \frac{V_s T_r}{P_r V_r}(P - P_0)$
Hohenberg	$V_{cyl}^{\frac{1}{3}}$	$C_m+1.4$
Assanis	L_c	$C_1 C_m + C_2 \frac{V_s T_r}{P_r V_r}(P - P_0)$
Hensel	$V_{cyl}^{\frac{1}{3}}$	$V = \frac{\sqrt{c_m^2 + c_c^2}}{2} + C_1 \frac{4\dot{m}_{air}}{\pi \rho_{air} B^2}(\frac{h_{IV,WOT}}{h_{IV}})^{C_2}$

Table 4. Coefficient of the models

Model	Coefficient			
	a	b	d	e
Annand	0.35-0.8	0.7	-	-
Woschni	0.013	0.8	-0.2	-0.53
Hohenberg	0.013	0.8	-0.2	-0.4
Assanis	0.013	0.8	-0.2	-0.73
Hensel	0.0656	0.8	-	-

4. Results and Discussion

To validate the simulation results, in Fig. 3., the results from numerical models were compared with the experimental work. The results which were presented in Figs. 3(a) and 3(b) were obtained in the air inlet temperature of 313K, the compression ratio of 12, the gasoline fuel octane number of 20, the engine speed of 800 rpm and 1200rpm, and an equivalence ratio of 0.62 and 0.53, respectively.

Figure 3 compares the experimental results and the results from the 0D-SZ simulation for the in-cylinder pressure and the RoHR. In the 0D-SZ simulations, the Annand, Woschni, Hohenberg, Assanis, and Hensel semi-empirical heat transfer models were employed. As it can be observed in Fig. 3., the 0D-SZ simulation results are in good agreement with the experimental data. For all of the used Semi-empirical heat transfer models, the RoHR results have a similar trend to the experimental data. Still the single-zone model over-predicts the maximum RoHR. This behavior occurs due to the assumptions of this model and the simultaneous combustion of the entire charge in the combustion chamber.

The ignition phenomenon in the HCCI engine depends on the changes in the in-cylinder temperature and pressure. Also, the SOC is directly affected by the air-fuel mixture and the in-cylinder gas temperature. As it was said, the used fuel in this study was a mixture of n-heptane and isooctane. Considering the different ignition of n-heptane and isooctane, the ignition of this mixture has two stages. The first stage is for the LTR-HR, and the second one is the HTR-HR. For better understanding and comparing the ignition phenomenon in different conditions and various equivalence ratios, in this study, the start of LTR-HR was considered as the time that the RoHR $(dQ/d\theta)$ reaches 3 J/deg. Also, the start of HTR-HR was considered as the time that the derivative of the RoHR $(d^2Q/d\theta^2)$ exceeds 40 J/deg^2. These definitions have been schematically presented in Fig. 4.

The experimental results of the RoHR and in-cylinder pressure for different equivalence ratios and different engine speeds have been illustrated in Fig. 5. Also, the start of LTR-HR and HTR-HR versus the equivalence ratio has been presented for various engine speeds.

Figure 5 shows that in the current experimental work, in the studied range, higher equivalence ratios increase the maximum RoHR and also the maximum in-cylinder pressure. This issue was predictable due to the higher fuel mass and higher heat release from the combustion. The results show that this trend exists in all of the studied engine speeds. These experimental results were considered as the comparison base for the examination of the 0D simulation.

Besides the maximum pressure and the RoHR, increasing the equivalence ratio advances both stages of the heat release. The start of LTR-HR and HTR-HR has been quantitatively presented in Fig. 5e.
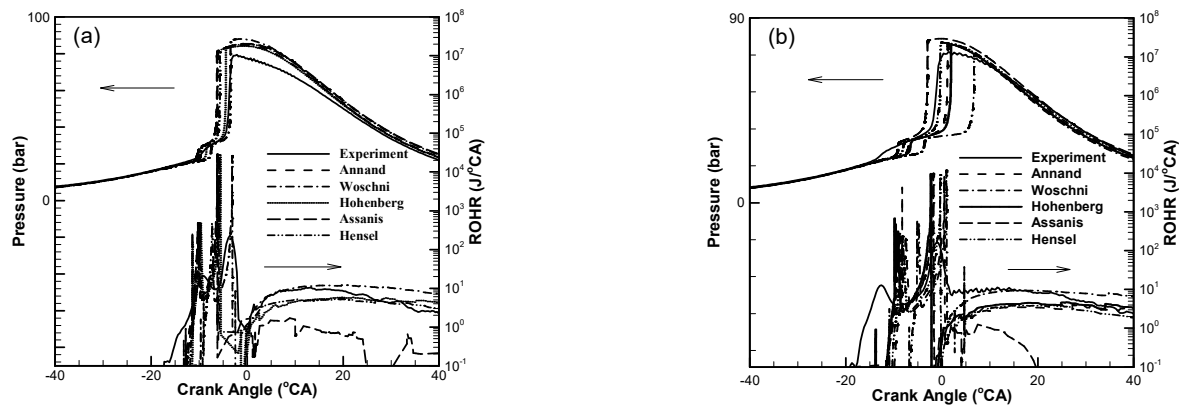

Fig. 3. Comparison of the RoHR and in-cylinder pressure with the 0D-SZ models and the experimental tests.
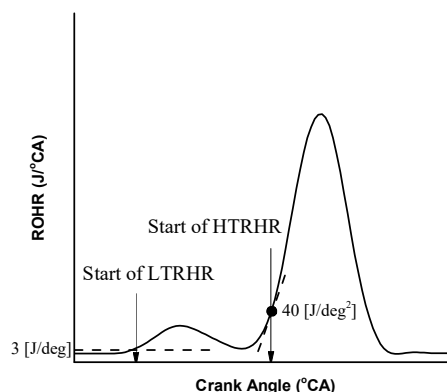

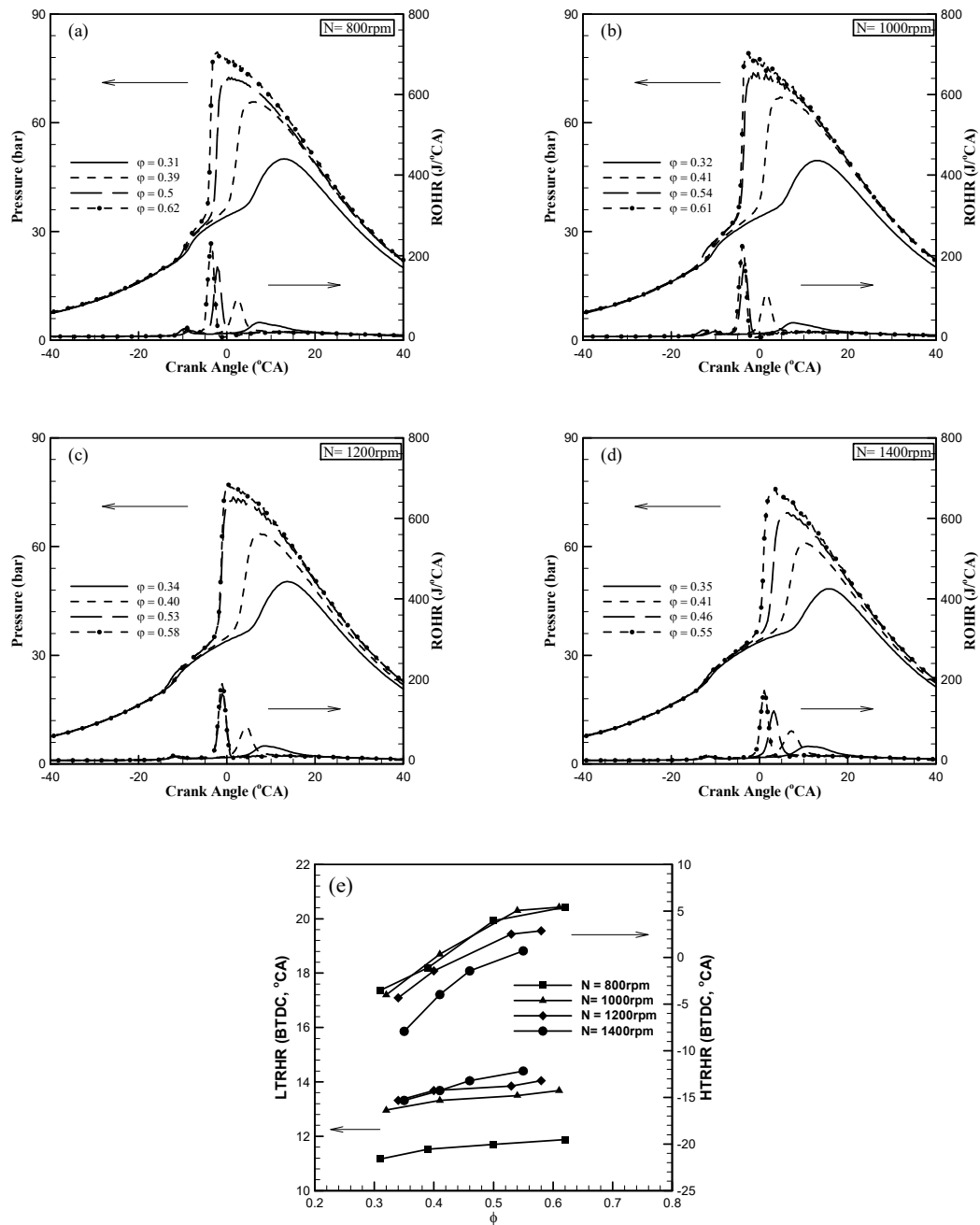**Fig. 4.** Definitions of the start of LTR-HR and HTR-HR.

Fig. 5. Experimental results for the RoHR and in-cylinder pressure versus crank angle in different equivalence ratios. a) N= 800 rpm, b) N= 1000 rpm, c) N= 1200 rpm, d) N= 1400 rpm, and e) Start of LTR-HR and HTR-HR versus equivalence ratio.

The 0D-SZ simulations for the changes in the RoHR and in-cylinder pressure versus the crank angle for different equivalence ratios and various engine speeds have been presented in Figs .6-9. In these figures, different heat transfer models, including the Annand, Woschni, Hohenberg, Assanis, and Hensel models, have been compared with each other. Also, in the f section of these figures, the start of LTR-HR and HTR-HR have been illustrated versus the equivalence ratio.

In the engine speed of 800 rpm (Fig. 6.), all of the semi-empirical heat transfer models saw the combustion process correctly. Furthermore, based on the plots, higher equivalence ratios, increase the RoHR and the in-cylinder pressure. In the experimental tests, it was recorded that by raising the equivalence ratio and with richer mixtures, the start of ignition happens earlier. As it can be found in Fig. 6f., by increasing the equivalence ratio, the Annand, Woschni, and Hohenberg models predict the start of LTR ignition contrariwise and more delayed. In contrast, the Assanis and Hensel models predict the effects of the equivalence ratio on the start of the first stage of ignition in an incorrect and disorganized way. With the rise of the equivalence ratio, the Annand and Hohenberg models correctly predicted the changes in the start of HTR ignition; however, the Woschni, Assanis, and Hensel models exhibited a disorganized and wrong behavior. Moreover, there are some irregularities in behavior of the Annand model when equivalence ratio increases and can be explained by the structure of the model. More specially, these irregularities occurred when equivalence ratio changed.

In the engine speed of 1000 rpm (Fig. 7.), all of the semi-empirical heat transfer models properly saw the LTR ignition, and these models (except Woschni's model for the equivalence ratio of 0.3) properly observed the HTR ignition. By increasing the equivalence ratio, the maximum pressure and RoHR increase. As it is shown in Fig. 7f., by enhancing the equivalence ratio, the Annand and Hohenberg models recognized the first stage of ignition contrariwise and more delayed. Also, the Woschni, Assanis, and Hensel models predicted the effect of the equivalence ratio on the start of LTR ignition in a wrong and disorganized way. With

the rise of the equivalence ratio, the Hohenberg model, correctly predicted the changes in the start of HTR ignition. In contrast, the Annand, Woschni, Assanis, and Hensel models exhibited an incorrect and disorganized behavior. As it was noted, Woschni's model did not see the HTR ignition in the equivalence ratio of 0.3; for this reason, in Fig. 7f., for this model, in the equivalence ratio of 0.3, the start of the second stage of ignition was not considered.

In the engine speed of 1200 rpm (Fig. 8.), all of the semi-empirical heat transfer models properly saw the first stage of the ignition. Also, all of the semi-empirical heat transfer models (except the Woschni model for the equivalence ratios of 0.34 and 0.4, and the Hohenberg model for the equivalence ratio of 0.34) properly observed the HTR ignition. All of the models (except the Assanis model) showed the raise of the maximum pressure and RoHR with rising the equivalence ratio. As it is illustrated in Fig. 8f., the Annand model recognized the start of the first stage of the heat release contrariwise and more delayed. By increasing the equivalence ratio, the Woschni, Hohenberg, Assanis, and Hensel models predicted the start of the LTR ignition incorrectly and disorganized. The effects of equivalence ratio on the start of the second stage of ignition were correctly predicted by the Annand, Woschni, and Hohenberg models, while the Assanis and Hensel models had a disorganized and wrong behavior. As it was stated, the Woschni model did not see the HTR in the equivalence ratios of 0.34 and 0.4, while the Hohenberg model was not able to observe this phenomenon in the equivalence ratio of 0.34. For this reason, these models did not consider the start of the second stage of heat release in Fig. 8f. Moreover, as it was explained, all of the semi-empirical heat transfer models properly showed the raise of the maximum pressure due to the rise of the equivalence ratio, and only the Assanis model was not able to predict this increase.
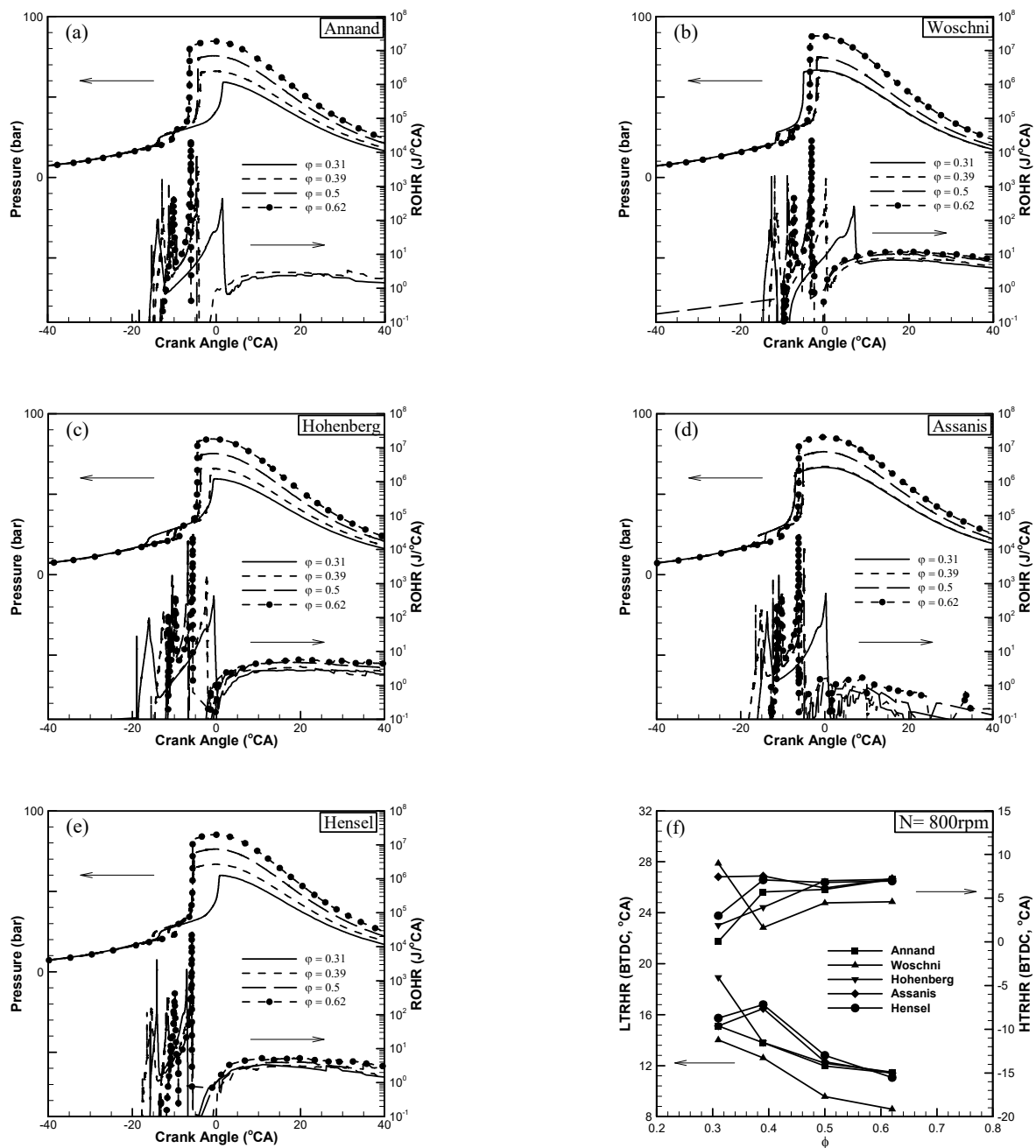

Fig. 6. In-cylinder pressure and RoHR versus crank angle for various equivalence ratios with the 0D-SZ models at N= 800rpm a) Annand, b) Woschni, c) Hohenberg, d) Chang (Assanis), e) Hensel and f) Start of LTR-HR and HTR-HR versus equivalence ratio.
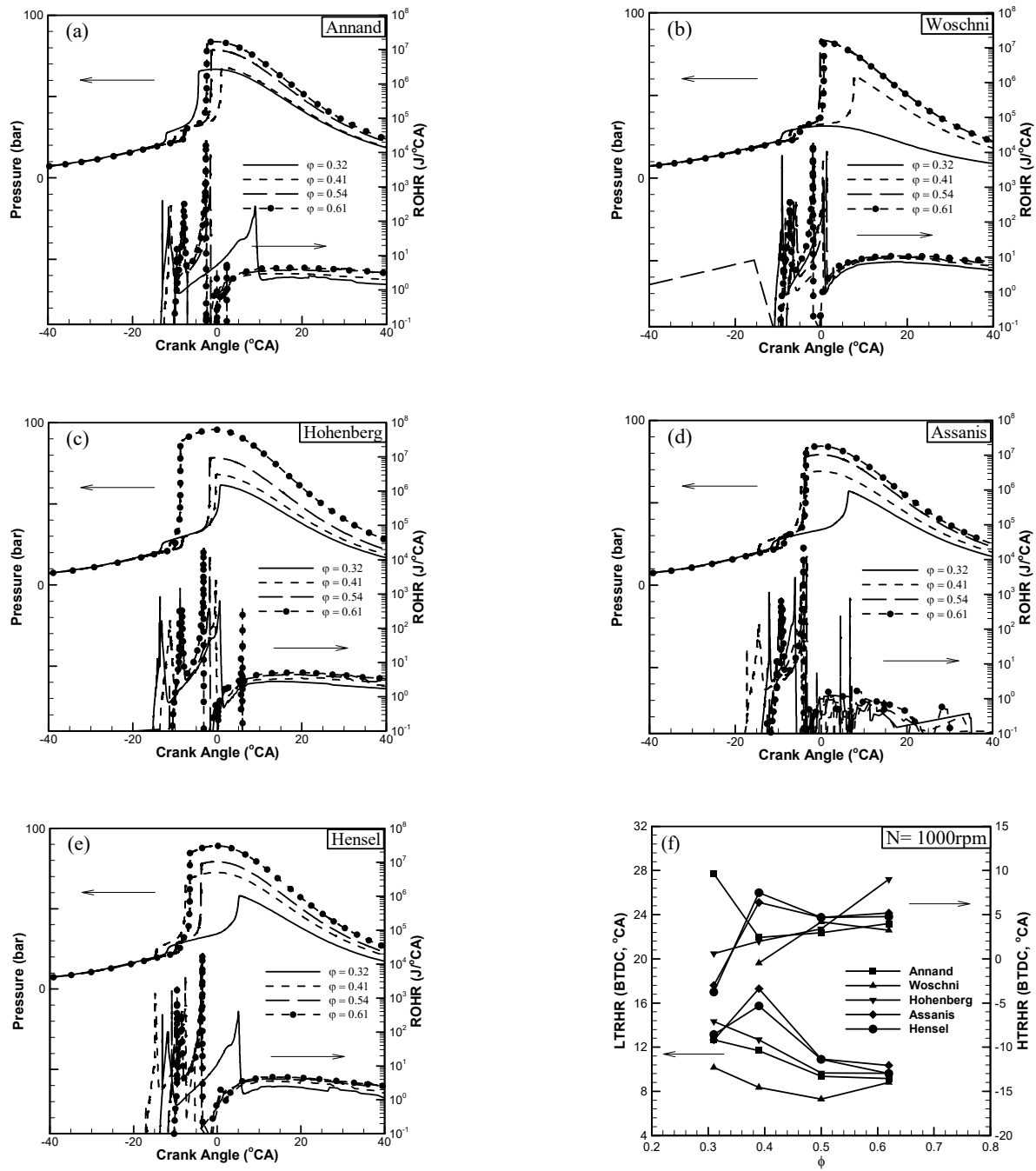
Fig. 7. RoHR and In-cylinder pressure versus crank angle for different equivalence ratios with the 0D-SZ models at N= 1000rpm a) Annand, b) Woschni, c) Hohenberg, d) Chang (Assanis), e) Hensel and f) Start of LTR-HR and HTR-HR versus equivalence ratio.

In the engine speed of 1400 rpm (Fig. 9.), all of the semi-empirical heat transfer models properly saw the first stage of the ignition. All of the semi-empirical heat transfer models (except Woschni's model in the equivalence ratios of 0.35, 0.41, and 0.46, and also Hohenberg's model in the equivalence ratios of 0.35 and 0.41) properly saw the second stage of the ignition. All of the models (except the Annand model) showed an increase in the maximum pressure and the RoHR with higher equivalence ratios. As it can be seen in Fig. 9f., the by increasing the equivalence ratio, the Annand and Woschni models recognized the start of LTR ignition contrariwise and more delayed. The Hohenberg, Assanis, and Hensel predicted the impacts of the equivalence ratio on the start of the first stage of heat release in a wrong and disorganized way. Among the semi-empirical models, only the Hohenberg model correctly predicted the influences of enhancing the equivalence ratio on the start of HTR ignition. As it was stated, the Woschni model was not able to see the second stage of ignition in the equivalence ratios of 0.35, 0.41, and 0.46, while the Hohenberg model did not observe this phenomenon in the equivalence ratios of 0.35 and 0.41. For this reason, in Fig. 9f., these models did not consider the start of HTR-HR in the above-mentioned equivalence ratios. Furthermore, as it was indicated, all of the semi-empirical heat transfer models properly showed the raise of the maximum pressure with the rise of the equivalence ratio, and only the Annand model was not able to properly predict this increase.
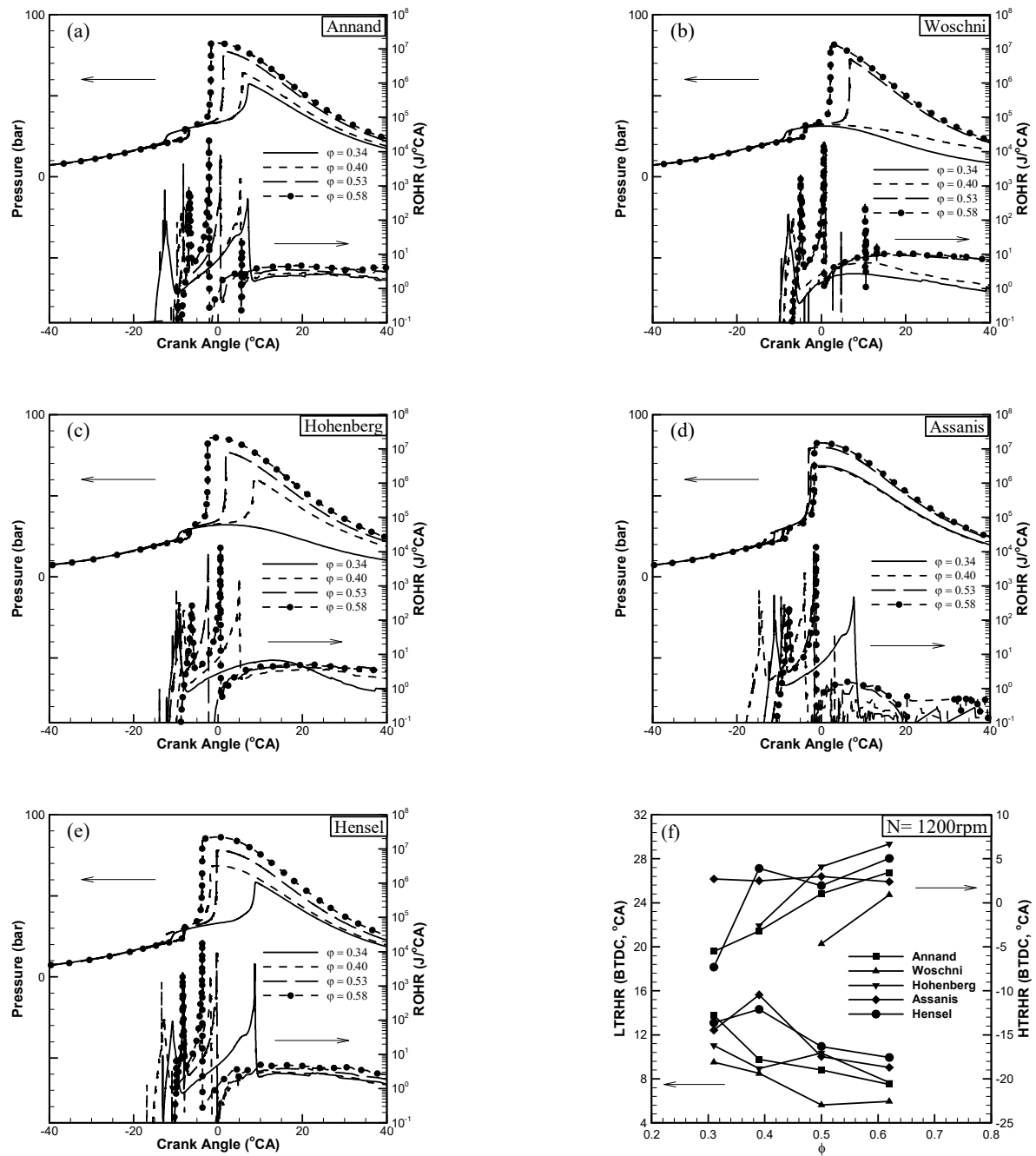
Fig. 8. RoHR and the In-cylinder pressure versus crank angle for various equivalence ratios with the 0D-SZ models at N= 1200rpm a) Annand, b) Woschni, c) Hohenberg, d) Chang (Assanis), e) Hensel and f) the start of LTR-HR and HTR-HR versus the equivalence ratio.

The summary of these results has been categorized in Table 5.

Table 5. The summary of the single zone zero-dimensional model results

Model	800 rpm		1000 rpm		1200 rpm		1400 rpm	
	LT	HT	LT	HT	LT	HT	LT	HT
Annand	#	+	#	~	#	+	#	~
Woschni	#	~	~	~	~	+	#	~
Hohenberg	#	+	#	+	~	+	~	+
Assanis	~	~	~	~	~	~	~	~
Hensel	~	~	~	~	~	~	~	~

+ : Correct prediction,   # : More delayed and contrariwise prediction, ~ : Incorrect and disorganized prediction, HT: High-temperature, LT: Low-temperature
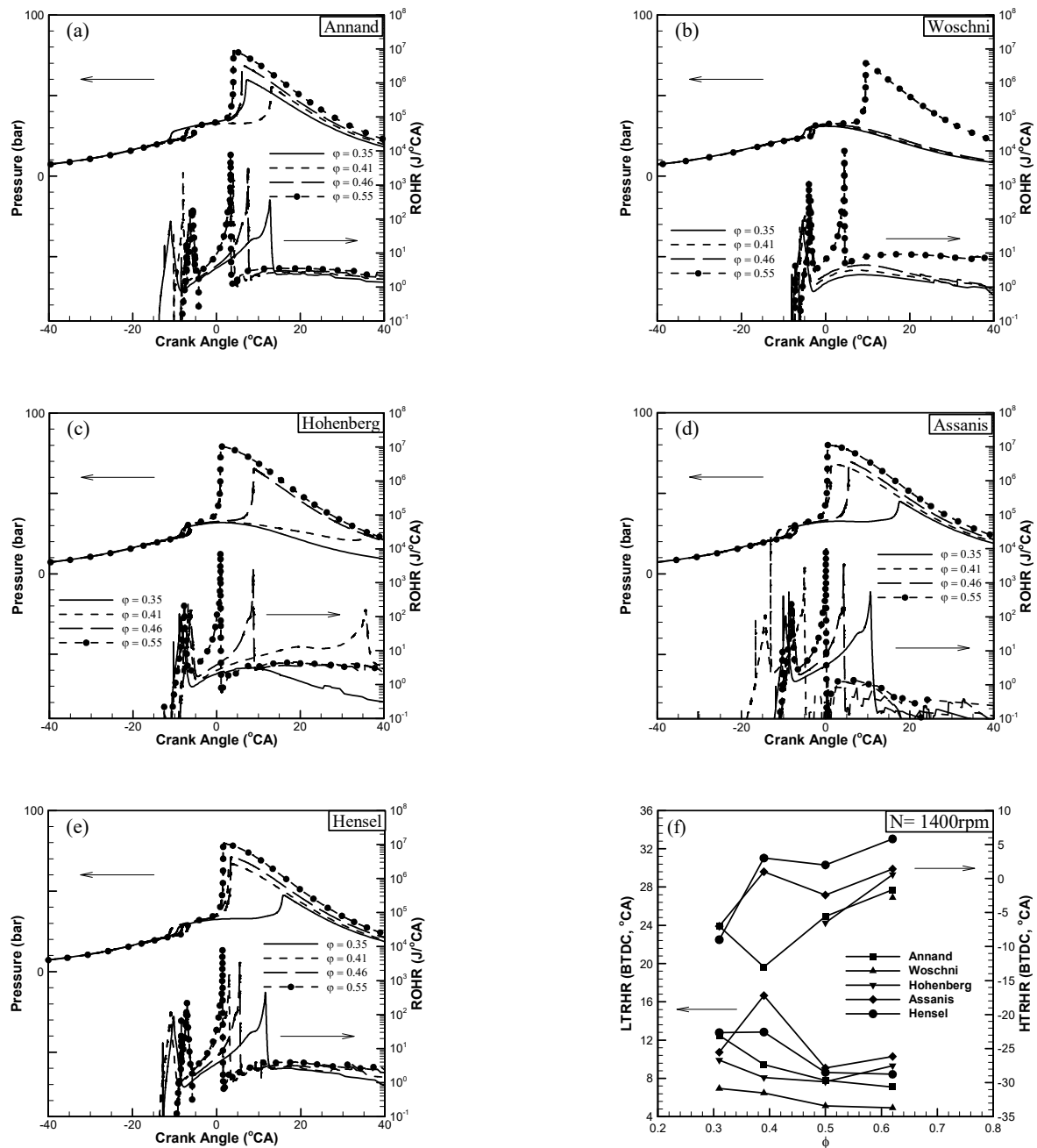
Fig. 9. RoHR and In-cylinder pressure versus crank angle for various equivalence ratios with the 0D-SZ models at N= 1400rpm a) Annand, b) Woschni, c) Hohenberg, d) Chang (Assanis), e) Hensel and f) Start of LTR-HR and HTR-HR versus equivalence ratio.

As it can be observed, the ability of the 0D-SZ model for predicting the heat release process of the fuels with two-staged heat release is significantly limited in different equivalence ratios. Even though changing the in-cylinder mixture in the 0D-SZ model leads to some changes in the temperature and pressure rise in the compression stage by affecting the thermodynamic properties such as the specific heat capacity, since it directly affects the heat transfer model, it seems that the models encounter with some problems in determining the exact SOC timing, especially for LTR-HR which is extremely temperature-dependent. Since in LTR-HR, a small portion of the total energy of the fuel is released, and also, the error is insignificant considering the expected precision of the models. It even changes by altering the definition of the start of LTR-HR, it can be concluded that this problem is neglectable. But on the other hand, this inability to predict the HTR-HR can considerably challenge the abilities of the models. The results show that in using the 0D-SZ model for evaluating the effects of the equivalence ratio, the Hohenberg model presents more reliable results.

5. Conclusions

In the present study, 16 different operating conditions of an HCCI engine was investigated to determine the effect of the equivalence ratio on LTR-HR and HTR-HR. The examinations were carried out by experimental test, and also 0D-SZ simulation by considering the chemical kinetics. In 0D-SZ simulation, different semi-empirical heat transfer models, including the Annand, Woschni, Hohenberg, Assanis, and Hensel models, were employed. The results of this research were as follows:

1. The experimental results showed that in the studied range, rising the equivalence ratio, enhances the maximum in-cylinder pressure and RoHR; also, it advances LTR-HR and the HTR-HR.
2. In the 16 studied operating conditions, the Annand, Assanis, and Hensel semi-empirical models were able to predict both stages of the combustion process; however, the Woschni and Hohenberg models could not recognize HTR-HR in some cases. With the dilution of the mixture and with higher engine speeds, the recognition of the start of HTR-HR by the Woschni and Hohenberg models became harder.
3. The rise of the maximum pressure due to the increase of the equivalence ratio was properly recognized by the Woschni, Hohenberg, and Hensel models. Still, the Assanis and Annand models did not recognize this increase in some cases.
4. All of the used semi-empirical heat transfer models had a wrong prediction for the effects of the equivalence ratio on the start of LTR-HR.
5. All of the semi-empirical heat transfer models except the Hohenberg model had an incorrect prediction for the effect of the equivalence ratio on the start of HTR-HR.
6. In all of the examined cases, the entire semi-empirical heat transfer models saw LTR-HR.
7. The Hensel model is the only model that saw the combustion and recognized the rise of the maximum pressure with the increase of the equivalence ratio properly, in all of the operating conditions.

Author Contributions

Masoud Rabeti principal investigator; Omid Jahanian sub-researcher (supervisor); Ali Akbar Ranjbar sub-researcher (supervisor); Seyed Mohammad Safieddin Ardebili sub-researcher (advisor); Hamit Solmaz sub-researcher. All authors approved the final version of the manuscript.

Acknowledgments

Conflict of Interest

The authors declare that there are no conflicts of interest that are relevant to current paper.

Funding

Data Availability Statements

The datasets generated and/or analyzed during the current study are available from the corresponding author on reasonable request.

Nomenclature

A	heat transfer surface area [m²]	Nu	Nusselt number
a, b, d, e	semi- empirical heat transfer coefficient	P	in-cylinder pressure [Pa]
B	cylinder bore [m]	Pr	Prandtl number
C_c	instantaneous piston speed [m/s]	Q	heat [J]
C_m	mean piston speed [m/s]	Q_{heat}	heat transfer from bulk gas to the cylinder wall [J]
C_p	heat capacity at constant pressure [J/KgK]	Re	Reynolds number
h	convective heat transfer coefficient [W/m²K]	r_c	compression ratio
h_{iv}	valve lift [m]	T	temperature [K]
k	thermal conductivity [W/mK]	V	volume [m³], characteristic velocity [m/s]
L	characteristic length [m]	V_d	displacement volume [m³]
N	engine speed [rpm]	V_s	swept volume [m³]

Greek Symbols

θ	crank angle [degree]	μ	viscosity [kg/m s]
γ	Specific heat ratio	ν	kinematic viscosity [m²/s]
ρ	density [kg/m³]		

References

[1] Asadi, A., Kadijani, O.N., Doranehgard, M.H., Bozorg, M.V., Xiong, Q., Shadloo, M.S., Li, L.K., Numerical study on the application of biodiesel and bioethanol in a multiple injection diesel engine, *Renewable Energy*, 150, 2020, 1019-1029.

[2] Fathi, M., Ganji, D.D., Jahanian, O., Intake charge temperature effect on performance characteristics of direct injection low-temperature combustion engines, *Journal of Thermal Analysis and Calorimetry*, 139(4), 2020, 2447-2454.

[3] Liu, W., Shadloo, M.S., Tlili, I., Maleki, A., Bach, Q.V., The effect of alcohol–gasoline fuel blends on the engines' performances and emissions, *Fuel*, 276, 2020, 117977.

[4] Leo, G.L., Sekar, S., Arivazhagan, S., Experimental investigation and ANN modelling of the effects of diesel/gasoline premixing in a waste cooking oil-fuelled HCCI-DI engine, *Journal of Thermal Analysis and Calorimetry*, 2020, 1-14.

[5] Geng, H., Wang, Y., Xi, B,. Li, Z., Zhen, X., Fu, C., Hu, Y., Study on HCCI combustion improvement by using dual assisted compression ignition (DACI) on a hydraulic free piston engine fueled with methanol fuel, *Applied Thermal Engineering*, 167, 2020, 114782.

[6] Ardebili, SM., Taghipoor, A., Solmaz, H., Mostafaei, M., The effect of nano-biochar on the performance and emissions of a diesel engine fueled with fusel oil-diesel fuel, *Fuel*, 268, 2020, 117356.

[7] Broekaert, S., *A study of the heat transfer in low temperature combustion engines*, Ph.D. Thesis, Ghent University, 2017.

[8] Onishi, S., Jo, S.H., Shoda, K., Do Jo, P., Kato, S., Active thermo-atmosphere combustion (ATAC)-a new combustion process for internal combustion engines, SAE *Technical paper*, 1979, No. 790501.

[9] Kim, DS., Lee, CS., Improved emission characteristics of HCCI engine by various premixed fuels and cooled EGR, *Fuel*, 85(5-6), 2006, 695-704.

[10] Ebrahimi, R., Desmet, B., An experimental investigation on engine speed and cyclic dispersion in an HCCI engine, *Fuel*, 89(8), 2010, 2149-2156.

[11] İpci, D., Yilmaz, E., Aksoy, F., Uyumaz, A., Polat, S., Solmaz, H., The Effects of iso-propanol and n-heptane Fuel Blends on HCCI Combustion Characteristics and Engine Performance, *Makine Teknolojileri Elektronik Dergisi*, 12(1), 2015, 49-56.

[12] Cinar, C., Uyumaz, A., Solmaz, H., Sahin, F., Polat, S., Yilmaz, E., Effects of intake air temperature on combustion, performance and emission characteristics of a HCCI engine fueled with the blends of 20% n-heptane and 80% isooctane fuels, *Fuel Processing Technology*, 130, 2015, 275-281.

[13] Cinar, C., Uyumaz, A., Solmaz, H., Topgul, T., Effects of valve lift on the combustion and emissions of a HCCI gasoline engine, *Energy Conversion and Management*, 94, 2015, 159-168.

[14] Calam, A., Solmaz, H., Yılmaz, E., İçingür, Y., Investigation of effect of compression ratio on combustion and exhaust emissions in A HCCI engine, *Energy*, 168, 2019, 1208-1216.

[15] Polat, S., Yücesu, HS., Kannan, K., Uyumaz, A., Solmaz, H., Shahbakhti, M., Experimental comparison of different injection timings in an HCCI engine fueled with n-heptane, *International Journal of Automotive Science and Technology*, 1(1), 2017, 1-6.

[16] Jahanian, O., Jazayeri, SA., A Numerical Investigation on the Effects of Using for Maldehyde as an Additive on the Performance of an HCCI Engine Fueled With Natural Gas, *International Journal of Energy and Environmental Engineering*, 173, 2011, 79-89.

[17] Fathi, M., Jahanian, O., Ganji, DD., Wang, S., Somers, B., Stand-alone single-and multi-zone modeling of direct injection homogeneous charge compression ignition (DI-HCCI) combustion engines, *Applied Thermal Engineering*, 125, 2017, 1181-1190.

[18] Namar, MM., Jahanian, O., Energy and exergy analysis of a hydrogen-fueled HCCI engine, *Journal of Thermal Analysis and Calorimetry*, 137(1), 2019, 205-215.

[19] Torregrosa, A.J., Olmeda, P.C., Romero, C.A., Revising engine heat transfer, *Journal of Engineering Annals of Faculty of Engineering Hunedoara*, 6(3), 2008, 245-265.

[20] Thermodynamics and Fluid Mechanics Group and Annand, W.J.D., Heat transfer in the cylinders of reciprocating internal combustion engines, *Proceedings of the Institution of Mechanical Engineers*, 177(1), 1963, 973-996.

[21] Woschni, G., A universally applicable equation for the instantaneous heat transfer coefficient in the internal combustion engine, *SAE Technical Paper*, 1967, No. 670931.

[22] Hohenberg, G.F., Advanced approaches for heat transfer calculations, *SAE Technical Paper*, 1979, No. 790825.

[23] Broekaert, S., De Cuyper, T., De Paepe, M., Verhelst, S., Evaluation of empirical heat transfer models for HCCI combustion in a CFR engine, *Applied Energy*, 205, 2017, 1141-1150.

[24] Chang, J., Güralp, O., Filipi, Z., Assanis, D.N., Kuo, T.W., Najt, P., Rask, R., New heat transfer correlation for an HCCI engine derived from measurements of instantaneous surface heat flux, *SAE Technical Paper*, 2004, No. 2004-01-2996.

[25] Hensel, S., Sarikoc, F., Schumann, F., Kubach, H., Spicher, U., Investigations on the heat transfer in HCCI gasoline engines, *SAE International Journal of Engines*, 2009, No. 2009-01-1804.

[26] Soyhan, H.S., Yasar, H., Walmsley, H., Head, B., Kalghatgi, G.T., Sorusbay, C., Evaluation of heat transfer correlations for HCCI engine modeling, *Applied Thermal Engineering*, 29(2-3), 2009, 541-549.

[27] Broekaert, S., De Cuyper, T., Chana, K., De Paepe, M., Verhelst, S., Assessment of empirical heat transfer models for a CFR engine operated in HCCI mode, *SAE Technical Paper*, 2015, No. 2015-01-1750.

[28] Broekaert, S., De Cuyper, T., De Paepe, M., Verhelst, S., Experimental investigation of the effect of engine settings on the wall heat flux during HCCI combustion, *Energy*, 116, 2016, 1077-1086.

[29] Heywood, J. B., *Internal Combustion Engine Fundamentals*, McGraw-Hill Book Company, 1988.

[30] Komninos, N.P., Rakopoulos, C.D., Heat transfer in hcci phenomenological simulation models: A review, *Applied Energy*, 181, 2016, 179-209.

[31] Jahanian, O., Jazayeri, SA., A comprehensive numerical study on effects of natural gas composition on the operation of an HCCI engine, *Oil & Gas Science and Technology–Revue d'IFP Energies Nouvelles*, 67(3), 2012, 503-515.

[32] Hairuddin, AA., Yusaf, TF., Wandel, AP., Predicting the combustion behaviour of a diesel hcci engine using a zero-dimensional single-zone model, *In: Proceedings of the 11th Australian Combustion Symposium (ACS 2011), Combustion Institute, Australian and New Zealand Section*, 1(1), 2011, 130-133.

[33] De Cuyper, T., Demuynck, J., Broekaert, S., De Paepe, M., Verhelst, S., Heat transfer in premixed spark ignition engines part II: Systematic analysis of the heat transfer phenomena, *Energy*, 116, 2016, 851-860.

[34] Wang, H., Yao, M., Reitz, RD., Development of a reduced primary reference fuel mechanism for internal combustion engine combustion simulations, *Energy & Fuels*, 27(12), 2013, 7843-7853.

ORCID iD

Masoud Rabeti https://orcid.org/0000-0002-1349-1051
Omid Jahanian https://orcid.org/0000-0002-5968-5185
Ali Akbar Ranjbar https://orcid.org/0000-0002-5244-1188
Seyed Mohammad Safieddin Ardebili https://orcid.org/0000-0002-5164-1284
Hamit Solmaz https://orcid.org/0000-0003-0689-6824

Publisher's Note Shahid Chamran University of Ahvaz remains neutral with regard to jurisdictional claims in published maps and institutional affiliations.